Solar Energy 231 (2022) 784–792

Contents lists available at ScienceDirect

Solar Energy

journal homepage: www.elsevier.com/locate/solener

Estimation of the effective nominal power of a photovoltaic generator under non-ideal operating conditions

José R. Angulo [a], Brando X. Calsi [a], Luis A. Conde [a], Jorge A. Guerra [a], Emilio Muñoz [b], Juan de la Casa [c], Jan A. Töfflinger [a,*]

[a] Science Department, Physics Section, Pontificia Universidad Católica del Perú, Lima, Peru
[b] IDEA Research Group (Research and Development in Solar Energy), Centre for Advanced Studies in Energy and Environment (CEAEMA), Department of Graphic Engineering, Design and Projects, University of Jaén, Spain
[c] IDEA Research Group (Research and Development in Solar Energy), Centre for Advanced Studies in Energy and Environment (CEAEMA), Electronics and Automation Engineering Department, University of Jaén, Spain

ARTICLE INFO

Keywords:
Solar photovoltaic systems
Measurement uncertainty
Statistical analysis
Condition monitoring
Nominal Power Estimation

ABSTRACT

The nominal power is an essential parameter for evaluating the general state of a photovoltaic plant. The American Society for Testing and Materials, the International Electrotechnical Commission and other works propose procedures that allow estimating the nominal power of a photovoltaic generator in outdoor conditions. These procedures generally require monitoring days with ideal conditions, particularly clear sky days with high irradiance values and low wind speeds. These restrictions can limit the available number of monitoring days, especially in places with frequent cloud formations.

In this work, a 109.44 kW photovoltaic plant was monitored for six months in Granada, Spain. Its nominal power is first estimated applying a referential procedure reported in the literature for large PV plants under the required ideal climatic conditions. In order to overcome the restrictions for estimating the nominal power, we propose a new procedure applicable not only for ideal but also for non-ideal conditions, such as found on partially cloudy days. This new procedure applies non-parametric statistics to find the most probable value of the nominal power within a single monitoring day. A statistical analysis indicates that it reliably estimates the nominal power at non-ideal conditions while preserving the same estimation accuracy as under ideal conditions.

1. Introduction

Energy transition policies towards renewable energy sources and decreasing solar electricity generation costs have pushed forward the growth of photovoltaic (PV) installations around the world. PV power generators are currently the third biggest installed renewable energy source after hydroelectric and wind power generators (REN21, 2021). Hence, the number of countries with more than 1 GW of additional PV power per year increased to 18 in 2020 (Jäger-waldau, 2021). Most of the additional PV power installed during the last decade originate from large-scale utility systems (Jäger-Waldau, 2019). One of the critical issues facing the PV industry is evaluating the PV plant (Rahman et al., 2018) and ensuring investors the value of the system through the implementation of International Standards (Kelly et al., 2014).

The specific yield and performance ratio (PR) are two parameters widely used by investors for bankability evaluations of such PV investments (Tina et al., 2017) since these parameters indicate the overall losses in a PV plant. The PR calculation requires meteorological data and the labeled nominal power (Shiva Kumar and Sudhakar, 2015). This nominal power (P^*_M) value is referred to as the generator's output power at the maximum power point under standard test conditions (STC), i.e., an irradiance of 1000 W/m^2, a module temperature of 25 °C and an AM1.5 spectrum according to the IEC 60904-3 standard (IEC 60904-3, 2008). Notable deviations of the PR from the expected value can be attributed to unexpected gains or losses in the PV plant. Such deviations can also be traced back to the difference between the labeled nominal power from the datasheet and the operational nominal power (Reich et al., 2012). Therefore, investors may request an onsite test of the operational nominal power with a report that includes a comparison between the as-built and as-planned state of the PV plant (Kiefer et al., 2011).

On the one hand, the American Society for Testing and Materials

* Corresponding author.
E-mail address: japalominot@pucp.edu.pe (J.A. Töfflinger).

https://doi.org/10.1016/j.solener.2021.12.015
Received 16 July 2021; Received in revised form 9 December 2021; Accepted 10 December 2021
Available online 20 December 2021

(ASTM) E2848-13 standard (E2848 –13, 2013) provides a procedure for determining the installed capacity or the maximum power output that a PV plant can produce at reporting conditions (RC). The RC are defined and agreed upon by the user; for instance, RC could be an irradiance equal to 1000 W/m^2, an ambient temperature equal to 20 °C and a wind speed equal to 1 m/s (Watts et al., 2017). In this case, the procedure requires measuring plane-of-array irradiance, ambient temperature, wind speed, and system power for at least three days. Then, multiple linear regressions are performed to fit the data of the aforementioned parameters to an empirical equation presented in the E2848-13 standard. Finally, this equation is evaluated at RC to obtain the capacity in kW or MW. Evidently, the standard does not recommend to apply this procedure for comparison of the capacity to the nameplate nominal power, i.e. to the P^*_M at STC.

On the other hand, the International Electrotechnical Commission (IEC) 61829 standard (IEC 61829, 2015) defines a procedure to characterize PV arrays by measuring the current–voltage (I-V) curve in outdoor conditions and then translating the measured maximum power to STC. This procedure provides information not only on the P^*_M but also on the essential electrical parameters available on the manufacturer's datasheet (Navada et al., 2017). Therefore, most of the P^*_M estimation methods of PV plants recommend the measurement of the I-V curve (Quiroz et al., 2015; Muñoz et al., 2011), when possible.

There are currently commercial instruments with the ability to trace the I-V curve of a PV generator but of power less than 100 kW. Therefore, to measure a higher power, each PV string must be characterized separately by measuring the I-V curve. Non-commercial alternatives use a capacitive load for the impedance variation. The load's capacity increases with the PV array size, making technical work more difficult since additional safety precautions must be taken into account at higher power (Muñoz et al., 2016; De la Parra et al., 2017).

In the absence of a clear international standard and using general-purpose instrumentation to evaluate the performance of electrical generation systems, Martínez-Moreno et al. (Martínez-Moreno et al., 2012) proposed a procedure for calculating the P^*_M of a PV generator; and successfully contrasted it with their results obtained by applying IEC 61829. This procedure determines the P^*_M in PV generators by monitoring the output power under the operating conditions.

The aforementioned norms given by the ASTM as well as the IEC, and the procedure presented in (Martínez-Moreno et al., 2012), require stable meteorological and operational conditions, such as clear sky with irradiance levels above 800 W/m^2 and low wind speeds. In this work, we refer to these conditions as "ideal". Furthermore, they require adequate measurement equipment (Carrillo et al., 2016), and a spectral mismatch correction should be performed when necessary. These strict conditions limit the applicability of monitored data, as depicted in Fig. 1. In this example, when looking for a day with the aforementioned ideal conditions, according to the ASTM E2848-13 standard, only the highlighted data (16.05.2018) fully complies with the standard. The photovoltaics for utility-scale applications (PVUSA) method based on the ASTM E2848-13 standard also requires collecting enough empirical data to satisfy a minimum of 10 h of solar irradiance above 1000 W/m^2 (Kimber et al., 2009). For most PV plants, such conditions may not occur, or it may take a long monitoring time to meet these requirements.

The other four days in Fig. 1 do not meet the requirements because they present substantial (12.05., 13.05. and 17.05.2018) or minor (15.05.2018) deviations from the clear sky irradiance conditions. These deviations introduce noise in the standards' procedures that can lead to incorrect estimates of P^*_M when applying the ASTM equations, the IEC standards, and the procedure applied in (Martínez-Moreno et al., 2012). These deviations observed on the other four days are mainly caused by the passage of clouds.

In this work, we propose a novel procedure that enables the inclusion of data from such non-ideal days to estimate the P^*_M. This procedure based on non-parametric statistics effectively identifies and filters out noise and deviations from ideal irradiance conditions and estimates the most probable P^*_M value with the remaining data for any day.

The proposed procedure enables the daily characterization of a PV plant without requiring that ideal conditions are fully met; thus, facilitating technical due diligence processes or quality control for newly installed plants or those involved in re-purchase processes. Daily monitoring of the P^*_M can also contribute to overseeing the PV plant's correct operation and evaluating the profitability parameters of the investment.

The paper is organized as follows; in Section 2, as a fundament of our work, we first briefly present the procedure suggested by Martínez-Moreno et al. (2012) and apply it to our data. Section 3 describes the experiment conducted in the PV plant and the monitoring system for our work. Section 4 highlights the main challenges observed in the PV generator under study, particularly a non-linear behavior of the power with irradiation causing a hysteresis effect. Section 5 shows the novel proposed procedure to calculate the probability density function with a non-parametric statistic. Finally, Section 6 shows the results of the novel procedure and their statistical analysis, followed by the conclusions of this research.

2. Fundament

Martínez-Moreno et al. (Martínez-Moreno et al., 2012) introduced a procedure relatively easy to understand and implement. As an initial step, the plane-of-array irradiance (G), module temperature (T_m) and DC power (P_{DC}) output are recorded every minute or quicker for at least one full day with irradiance levels above 800 W/m^2.

The second step of the procedure suggests translating the measured

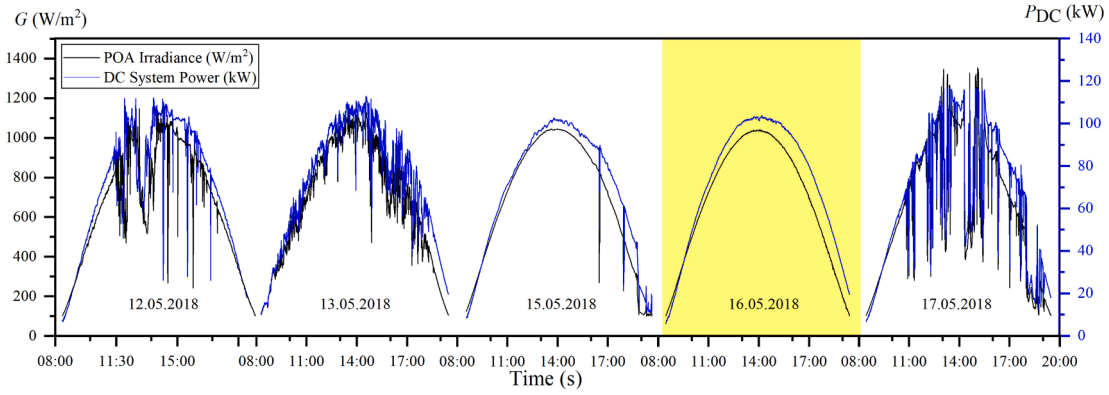

Fig. 1. Example of measurements every 30 s of plane-of-array irradiance and DC power output for five days. According to the ASTM E2848-13 standard, only the one day marked in yellow (16.05.2018) fully meets the requirements for estimating the nominal power.

DC output power to the DC power temperature-corrected to 25 °C ($P_{DC} \rightarrow P_{(G,T\rightarrow 25^{\circ}C)}$), defined as

$$P_{(G,T\rightarrow 25^{\circ}C)} = \frac{P_{DC}}{\left(1+\gamma\left(T_m - T_m^*\right)\right)} \quad (1)$$

where γ is the power temperature coefficient provided by the manufacturer (in %/°C), T_m^* is the module or cell temperature at STC (25 °C).

As stable weather conditions are required, as shown in Fig. 1 for the irradiance, the irradiance measured in step 1 has to be restricted to values between 800–1000 W/m^2 to avoid errors emerging from inverter saturation and non-linear PV module efficiency dependence on the irradiance (Whitfield and Osterwald, 2001).

Finally, as seen in Fig. 2, the slope of the linear regression (800–1000 W/m^2) gives the nominal power P_M^*, through:

$$P_{(G,T\rightarrow 25^{\circ}C)} = P_M^* \times \frac{G}{G^*} \quad (2)$$

Here, G* is the irradiance at STC (1000 W/m^2). Hence, by performing a linear global fit, one can obtain P_M^* with data from a single day.

This procedure satisfactorily verifies P_M^* of an installed PV generator. However, it requires the aforementioned weather conditions, particularly clear-sky, thus, excluding those days during the monitoring process that do not satisfy these conditions, for example, due to partial cloud formations. The purpose of the following work is to extend the procedure to estimate P_M^* even for those days that do not fully meet these conditions.

3. Experimental details

In this work, the experimental facility is a 109.44 kW grid-connected PV plant located in Granada, Spain (Latitude: 37.287, Longitude: −3.057) (Muñoz-Cerón et al., 2018). The commercial PV plant has been connected to the grid in 2008 and has been operational since then. Fig. 3 shows ground (top) and satellite (bottom) photos of the system under study. The main electrical characteristics are summarized in Table 1. The PV generator initially worked on two tracking axes. However, during the experimental campaign, all trackers were fixed facing South and tilted at 30º. It should be noted that not all the PV arrays are identically aligned and co-planar, as seen in the photos. We estimated an alignment difference of up to 10° between array orientations from the satellite image. This misalignment is due to uncertainties in the axes' mechanical positioning and the mounting ground's unevenness.

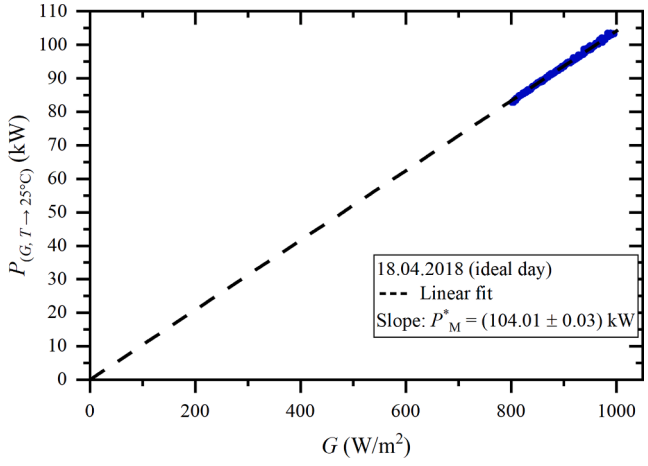

Fig. 2. Example of a day (18.04.2018) that meets the required test conditions according to (Martínez-Moreno et al., 2012). The DC power temperature-corrected to 25 °C versus irradiance is presented. The slope of the global fit of the data yields the nominal power P_M^*.

The monitoring of the PV generator is carried out by measuring the operating conditions (irradiance and module temperature) and the DC power at the maximum power point (MPP) in the inverter.

Our data acquisition system recorded the plane-of-array irradiance (G) with a calibrated PV module of the same technology and spectral response as the modules of the PV generator under inspection (Polo et al., 2017). Furthermore, the PV module was installed at the same angle and orientation as the adjacent string near the geometric center of the PV generator. In Fig. 3, bottom image, the position of the calibrated module, aligned to the adjacent string, is indicated by an arrow.

The irradiance measurement quality that effectively impinges on the PV generator is affected by both the uncertainty related to the value of the short-circuit current of the calibrated PV module (1.8 %, according to the calibration certificate) and that related to the shunt resistance (0.5 %, according to the manufacturer's specifications). The uncertainty introduced by the resolution of the datalogger (analog–digital conversion-16 bits, with a full scale of 100 mV) and the accuracy of this device (0.1 % of a 100 mV-full scale) is negligible in this uncertainty budget.

The module temperature (T_m) can be indirectly measured through open-circuit voltage measurements of a calibrated module (Huang et al., 2011), or by infrared images of the PV module using a thermal imaging camera (Irshad and Haque, 2018), or by sensors (PT100 or thermocouple) located at the module backside (Barykina and Hammer, 2017). For the PV generator under study, the T_m was recorded with one J-type thermocouple sensor placed on the back side of a PV module under operating conditions (Muñoz-Cerón et al., 2018).

This PV module was part of the string adjacent to the irradiance sensor near the geometric center of the PV generator. It should be noted that the T_m measurements were conducted at the same module under operating conditions throughout the experimental campaign.

Regarding the quality related to the T_m measurements, it is affected by both the uncertainty due to the accuracy of the J-type thermocouple (± 1.5 °C, according to the manufacturer's specifications), and the uncertainty due to the accuracy of the datalogger (± 1.7 °C, according to the manufacturer's specifications).

Finally, the DC power at the inverter input was measured with a calibrated YOKOGAWA WT1600 wattmeter, which has an uncertainty of less than 0.5 %. As recommended in (Martínez-Moreno et al., 2012), the irradiance, module temperature, and DC power were acquired every 30 s from March 27th to September 30th, 2018.

According to the module manufacturer's datasheet, the nominal power of the generator at STC is 109.44 kW. For reference, in a prior study (Lomas, 2019), each string of this PV generator was characterized through I-V curve measurements. By extrapolation to STC following the IEC 61829 standard, the P_M^* of the entire plant was estimated at 103.90 kW, with a standard deviation of 1.2 %. Compared to the manufacturer's value, the theoretical loss represents a decrease of 4.9 % in 10 years after its installation in 2008. This difference could be attributed to an annual degradation of ~ 0.5 % of the polycrystalline panels (Jordan and Kurtz, 2013; Carullo et al., 2014), resistive wiring losses and/or module/string mismatch (Lorente et al., 2014), among other causes.

During the monitoring period of six months, 39 out of 135 days with reliable monitoring data complied with the required operating conditions for the Martínez-Moreno et al. (Martínez-Moreno et al., 2012) procedure. Fig. 4 presents the resulting daily estimations of the nominal power and their deviation in % from their mean value. The mean value of P_M^* for the 39 days is 103.97 kW with a standard deviation of 0.77 kW and deviations from the mean value below ± 2 %. These values agree very well with the findings in the study performed in (Lomas, 2019).

4. Identified challenges in PV generator monitoring and data evaluation

We identified different challenges in monitoring the operating

Fig. 3. The 109.44 kW grid-connected PV plant located in Granada, Spain. Top: Photo taken at ground level. Bottom: Satellite photo (Latitude: 37.287, Longitude: −3.057).

Table 1
Main characteristics of the PV plant with DC electric parameters at STC according to module datasheet.

Characteristics of the PV generator	
Current at the maximum power point (A)	257.60
Voltage at the maximum power point (V)	574.20
Power at maximum power point (kW)	109.44
Power temperature coefficient (%/°C)	−0.43
Number of modules per string connected in series	18
Number of strings connected in parallel	32

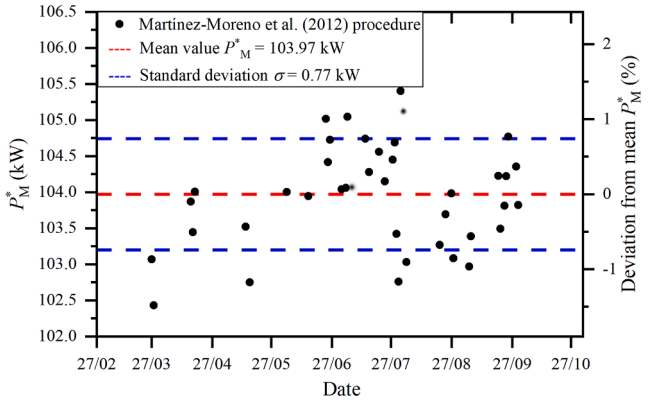

Fig. 4. Daily nominal power values according to the procedure presented in (Martínez-Moreno et al., 2012). The mean value and the standard deviation of P^*_M the for the 39 days are indicated.

conditions during the experimental campaign, which contribute to uncertainties in evaluating the PV generator's operating conditions and electrical parameters. For instance, the measurement of the operating temperature of a module does not represent the operating temperature for the entire plant and is one of the biggest challenges in PV monitoring. With randomly changing speeds and directions, winds can promote operating temperature inhomogeneities and temporally instantaneous or delayed temperature gradients of up to 10 °C in the same PV plant (Muñoz Escribano et al., 2018). Therefore; single local temperature measurements in a PV generator seldomly represent the entire generator's average temperature, thus increasing the measurement's uncertainty.

Further inhomogeneities in a PV generator derive from slightly different aligned strings. Such misalignments may arise from the uneven ground or slightly different mounting structures, as in most plants such as the one under investigation in Fig. 3. Consequently, different strings may capture distinct levels of plane-of-array (POA) irradiance simultaneously. Therefore, the local irradiance measurements in a PV generator may not represent the irradiance captured by the entire generator, thus, introducing an additional source of uncertainty.

Fig. 5(a) shows the monitored data (POA irradiance, module temperature, and DC power) for an exemplary day with ideal operating conditions. There seems to be a good alignment between irradiance and DC power data during morning hours. However, there is a temporal delay between these two parameters during afternoon hours. This delay is caused most likely by a misalignment between the irradiance sensor and some strings. The bottom photo in Fig. 3 shows that the string used to align the calibrated module is slightly differently oriented than some of the other PV plant's strings. The possibility of minimizing the impact of this misalignment was evaluated by estimating the mean orientation of all strings and placing the irradiance sensor in this mean orientation. However, for this experimental campaign, it was decided to follow precisely the characterization protocol proposed in (Martínez-Moreno et al., 2012) and to take advantage of this particular circumstance to analyze the protocol's validity when applied in a PV plant with non-ideal characteristics during an extended campaign that has entailed its application in very different weather conditions. Furthermore, this drawback allowed us to verify the robustness of this work's proposed analysis method of the experimental results. Therefore, and as previously mentioned, we installed both the irradiance sensor and a single sensor for measuring module temperature in the string that occupies the

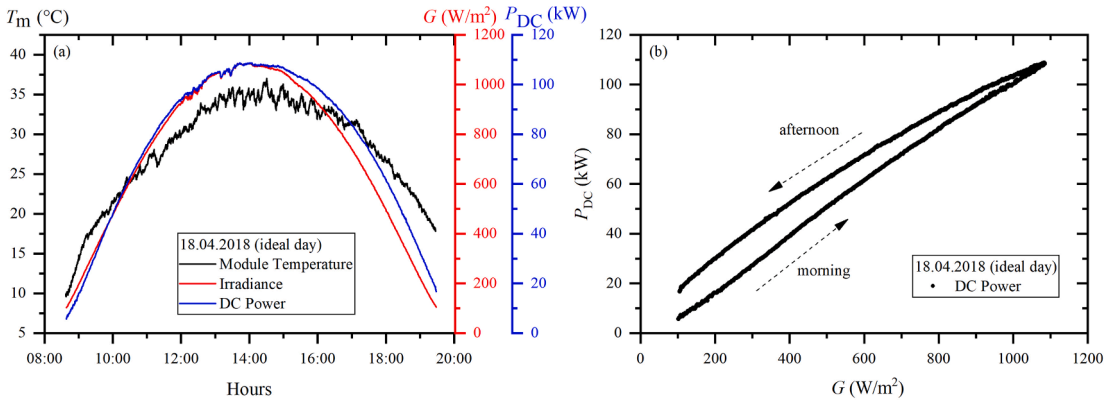

Fig. 5. (a) Plane-of-array irradiance, module temperature, and DC power for a sunny day with ideal conditions (18.04.2018). (b) DC power versus irradiance shows a hysteresis effect due to linear and non-linear behavior in the morning and afternoon, respectively.

geometric center of the PV generator.

Furthermore, in Fig. 5(a), we observe a temporary delay in the module temperature registering higher module operating temperatures during the afternoon at the same irradiance levels as in the morning. This temporal asymmetry of the module's temperature can originate from varying wind conditions and different heating and cooling speeds during the morning and afternoon.

A single irradiance sensor and a single module temperature sensor evidently may not offer us exact information on the actual operating conditions of the entire set of modules that make up the PV generator. This limitation can impact the relationship between the PV plant's power and the measured operating conditions. For example, in Fig. 5(b), the DC power first shows a quasi-linear response to the irradiance from morning to noon and, then, a non-linear response in the afternoon resulting in a counter-clockwise hysteresis formation.

In (Filik et al., 2018), this non-linear behavior was demonstrated for averaged irradiance, ambient temperature, and power values on a small system level (3 kW) and described as a hysteresis effect attributed to temporal delays in the response of the power to temperature changes (cooling and heating) during the morning and afternoon. However, in our case, if the temperature were the dominating factor for the hysteresis formation, we would expect lower DC power values in the afternoon for higher temperature values at the same irradiances, assuming that as suggested in (Martínez-Moreno et al., 2012), the estimation of the operating temperature of the entire PV generator can be approximated by one of its modules located at a strategic point in the plant. This would result in a clockwise hysteresis. Instead, we observe a counter-clockwise hysteresis in Fig. 5(b). Therefore, it seems a reasonable hypothesis for this particular case that the hysteresis formation is predominantly affected by the uncertainty in the irradiance measurement due to the misalignment of the numerous PV strings. These misalignments give rise to different angles of incidence between our irradiance sensor and some of the photovoltaic arrays (Carrillo et al., 2016). However, we do not rule out a temperature contribution to the hysteresis because the experimental values registered by the single sensor cannot consider possible inhomogeneities of the temperatures of the modules that make up the entire PV generator.

Therefore, to calculate the nominal power, we take into account only the quasi-linear region of the power output for irradiances > 800 W/m^2 from morning to noon following the procedure explained in Section 2. For this standard procedure to estimate the nominal power, it is crucial to omit the non-linear part of the hysteresis data since this data from the afternoon may not represent the correct operation of the PV plant. However, in the next section, we propose a new procedure to estimate the P^*_M by filtering out any effects that make the estimation difficult and introduce noise. This new procedure is based on non-parametric statistics. Other works in PV have applied non-parametric statistics, for instance, to predict the PV output power through time series analysis (Ren et al., 2014).

5. Non-Parametric statistical filtering process

A given group of N measurements in an experiment {X = x_1, x_2, …. …, x_N} can be represented by its mean (μ) and standard deviation (σ). The hypothesis is that the N measurements' values correspond to one parameterized distribution family, for example, a normal or Gaussian distribution. Such parametric statistics are a widely used and perfectly valid approach providing valuable information.

In PV, the data corresponding to a parametric statistic usually comes from a controlled environment, such as a laboratory. However, the observables are more likely to be affected by additional random effects during the experiment under outdoor conditions. For instance, a cloud or an increase in wind speed may generate inhomogeneities in irradiance and module temperature, which experimentally are almost impossible to consider or predict. This can lead to anomalies and/or artifacts in the data, power, irradiance, and module temperature, thus enhancing the modeling error. Therefore, the P^*_M estimation methods require the ideal climatic conditions considered in the characterization procedures mentioned previously.

From a statistical point of view, these random noise values can be identified by calculating the probability distribution function (PDF). The purpose of the following is to demonstrate that the PDF calculation can be a tool to calculate the nominal power.

To do so, we define the instantaneous nominal power P^i_M for an *i-th* data set:

$$P^i_M = P_{(G,T\to 25^\circ C),i} \times \frac{G^*}{G_i} \tag{3}$$

In Fig. 6(a), the temperature-corrected DC power $P_{(G,T\to 25^\circ C)}$ over the POA irradiance G for the exemplary ideal day (18.04.2018) is depicted. The hysteresis formation remains here, indicating that it is caused by the array misalignments rather than temperature anomalies. Using Eq. (3), we calculate the respective local nominal power P^i_M for each set of data points i, however, only for irradiance values > 800 W/m^2 where the most linear behavior is expected. Fig. 6(b) presents the histogram of the resulting P^i_M values for this particular day. The histogram shows a non-normal distribution with multiple nodes or distribution peaks, indicated by black arrows. Hence, it becomes evident that an approach to calculate unknown or non-parametric probability distributions is needed.

An unknown PDF can be calculated by applying a kernel density estimation (KDE) (Nosratabadi et al., 2019). The KDE can be expressed as

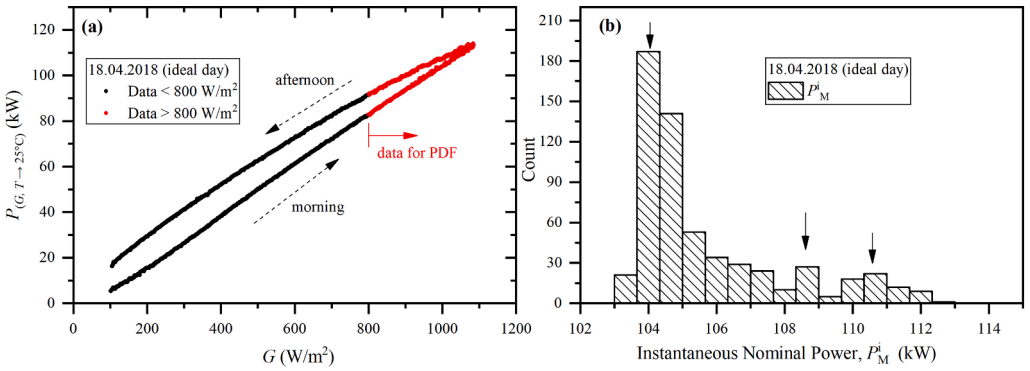

Fig. 6. (a) Temperature-corrected DC power versus irradiance for a sunny day with ideal conditions (18.04.2018). The hysteresis effect is observable. Data for probability density analysis is marked in red. (b) Corresponding histogram of the instantaneous nominal power values P^i_M calculated for irradiances > 800 W/m^2. The black arrows indicate the three local maxima of this histogram.

$$\widehat{f}_{(p)} = \frac{1}{nh}\sum_{i=1}^{n} K\left(\frac{p-p_i}{h}\right) \tag{4}$$

Where $\widehat{f}_{(p)}$ is the estimated probability density, n represents the sample size, h is the bandwidth, also called a smoothing parameter, $K_{(z)}$ is the kernel function of z, p_i is the random variable, and p is the mean of the set of values in n. For our purposes, we consider $p_i = P^i_M$

The kernel function and the bandwidth are critical parameters that determine the shape of the PDF. Therefore, their implementation carried out in this work will be briefly explained. The kernel function $K_{(z)}$ is the base function that keeps counts of the P^i_M. The simplest kernel, $K_{(z)} =$ *boxfunction*, is presented in the histogram of Fig. 6 (b). However, this central rectangular function is a discontinuous or non-uniform function, making it challenging to identify the probability peaks. The proper kernel that smooths the curve is the Gaussian function (Han et al., 2019), which will be considered here.

The bandwidth has a significant effect on the smoothing of the KDE (Rawa et al., 2011). In Fig. 7, low values (e.g., $h = 0.02$ kW) can generate many oscillations in the PDF. On the other hand, high values (e.g., $h = 2.00$ kW) flatten the curve, making it challenging to identify the distribution's peaks.

A common approach to select the most suitable bandwidth for unimodal data or data close to the normal distribution is Silverman's rule (Chen, 2017). However, for data distributions that are multimodal or far from a normal distribution, as in our case, the Improved Sheather-Jones (ISJ) algorithm is applied to find the optimal bandwidth (Chen, 2017), which for this particular day is $h = 0.115$ kW. This facilitates the identification of one main peak and several minor peaks. We propose that the mode, the value with the highest probability density, is the representative value for the effective nominal power under operating conditions. For this particular clear sky day, we get the mode $P^*_M = 103.96$ kW. This value is very close to the referential value $P^*_M = 104.01$ kW in Fig. 2 when following the procedure in (Martínez-Moreno et al., 2012) for the same day. Furthermore, it can be assumed that the minor peaks are related to noise, outliers, and/or non-linear hysteresis data. Consequently, the proposed procedure identifies the most probable nominal power value in one day and filters out the other values with lower probability.

Summarizing the steps mentioned above, we estimate the effective nominal power as follows:

1. $p_i = P^*_{M,i}$ is the input data in the kernel estimator for G > 800 W/m^2.
2. For the PDF, the smoothed $K_{(z)}$ is a Gaussian function.
3. The optimal bandwidth or smoothing parameter h is calculated through the ISJ algorithm.
4. The mode of the resulting PDF is considered the representative P^*_M.

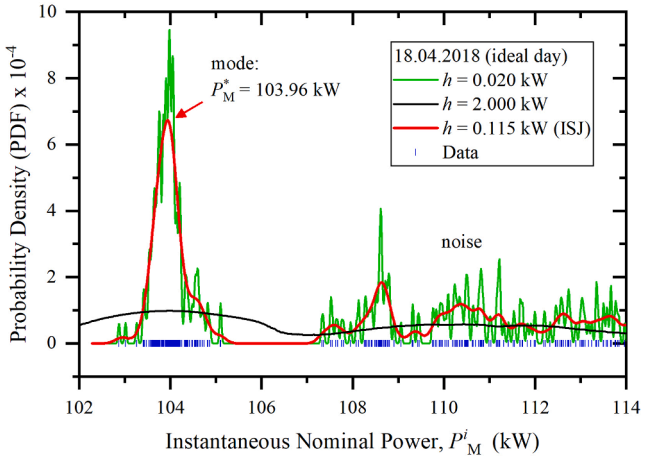

Fig. 7. The probability density functions PDF for three different bandwidths applied on the same dataset (18.04.2018) at irradiances > 800 W/m^2. The PDF with optimal bandwidth $h = 0.115$ kW is obtained via the ISJ algorithm. The red arrow indicates the mode to be considered as the PV generator's representative nominal power for this particular day. The noise originating from the hysteresis is indicated.

Of the 135 days with reliable monitoring data, 96 days did not comply with the operating conditions required by the Martínez-Moreno et al. (Martínez-Moreno et al., 2012) procedure. To demonstrate the applicability of the proposed procedure in this work for these 96 days with non-ideal operational conditions, we perform the aforementioned steps for an exemplary cloudy day with relatively few instances of high irradiance. Fig. 8(a) shows the plane-of-array irradiance, module temperature, and DC power of such a predominantly cloudy day. High irradiance values (G > 800 W/m^2) can be observed occasionally. Notwithstanding, the crossing of the clouds introduces fluctuating irradiance and module temperature values and most likely additional inhomogeneities in the POA irradiance between strings and irradiance sensor due to partial shadowing. In Fig. 8(b), this translates to considerable noise in the corresponding relation between $P_{(G,T\to25^\circ C)}$ and G. It is evident that this data cannot be represented by a single adequate global linear regression, thus, the procedure by (Martínez-Moreno et al., 2012) is not applicable.

However, in Fig. 9(a), following the aforementioned steps of the PDF calculation for this exemplary day with non-ideal conditions (30.04.2018), the resulting non-parametric statistic shows a mode with a value of $P^*_M = 103.53$ kW. This value is very close to one calculated for the clear-sky day (18.04.2018), $P^*_M = 103.96$ kW. The probability density distribution for the day with non-ideal conditions is much

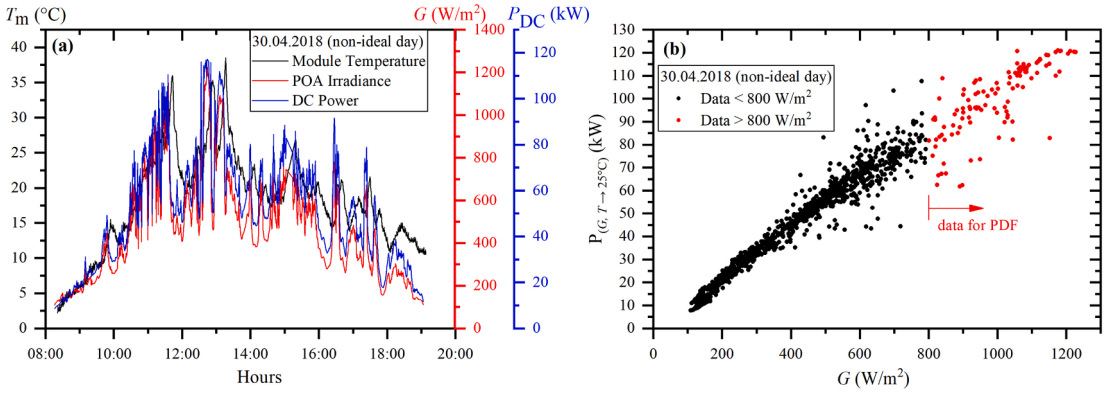

Fig. 8. Exemplary case of a non-ideal, partially cloudy day (30.04.2018). (a) Plane-of-array irradiation, module temperature, and DC power for the full day. (b) The temperature-corrected DC power versus irradiance. Data sets at irradiances > 800 W/m^2 for probability density analysis are marked red.

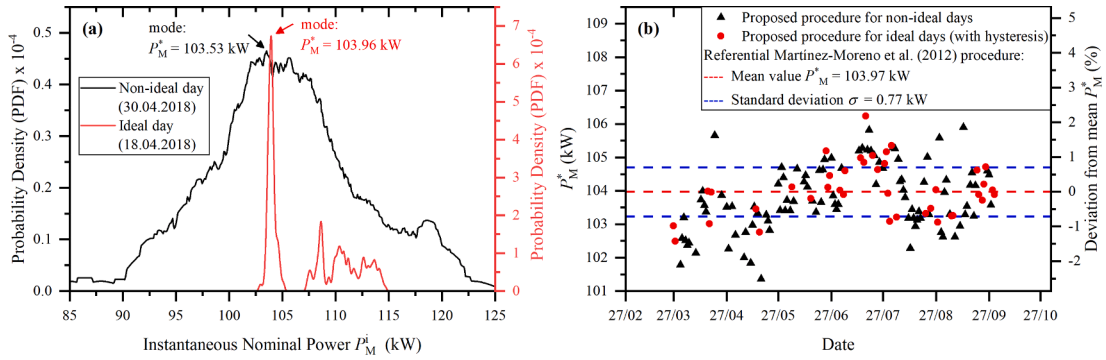

Fig. 9. (a) Probability density function (PDF) for an exemplary cloudy day (30.04.2018) with non-ideal conditions, compared to the clear-sky day with ideal conditions (18.04.2018). The modes marked by arrows represent the nominal power with the highest probability. (b) Daily nominal power values with the highest probability (modes) for ideal and non-ideal conditions.

broader than for the day with ideal conditions, which is a consequence of the noise created by the clouds. The difference between their two P^*_M values is 0.43 kW (0.41 %) which is within the standard deviation calculated in clear sky conditions 0.77 kW (0.74 %) and is less than the uncertainty of the power measurement of 0.5 %. This small difference indicates that the proposed procedure enables the reliable estimation of the P^*_M for this particular non-ideal day.

Fig. 9(b) depicts the nominal power calculated according to this work's proposed procedure for the 135 days during our experimental campaign. The hysteresis data has been included for both cases, with the only restriction being $G > 800$ W/m^2. Values of P^*_M for days with non-ideal conditions are marked in black, and for days with ideal conditions are marked in red. Their deviation in % from the mean value of $P^*_M = 103.97$ kW resulting from the reference procedure by Martínez-Moreno et al. (2012) is indicated. The P^*_M values are centered around this mean value. Most values are within the standard deviation of 0.77 kW or 0.74 %. Some values reach deviations of up to ± 2.5 % from the mean P^*_M, for days with and without ideal conditions. However, these deviations are within a reasonable range considering the measurement uncertainties described in chapter 3, and that strictly following the reference procedure for ideal days yields uncertainties up to ~ 2 % in Fig. 3.

6. Result and discussion

To validate the applicability of the proposed procedure, we perform a statistical analysis of the resulting daily nominal power values of the PV plant. As reference and case (1), we have the procedure already established by Martínez-Moreno et al. (Martínez-Moreno et al., 2012), which can be applied only for clear-sky days in ideal conditions and requires excluding non-linear data from the hysteresis. Then, as case (2), the proposed procedure with the non-parametric filter is tested with the same data set for clear-sky days; this case, however, also includes the non-linear data from the hysteresis effect. Finally, as case (3), the proposed procedure is also statistically evaluated for partially cloudy days under non-ideal conditions. Fig. 10 presents all estimated daily values of the nominal power in a boxplot analysis. Table 2 summarizes the main statistical parameters.

For case (1), in the black points, the P^*_M values were calculated for the 39 days with ideal conditions. In the black line, daily values indicate a

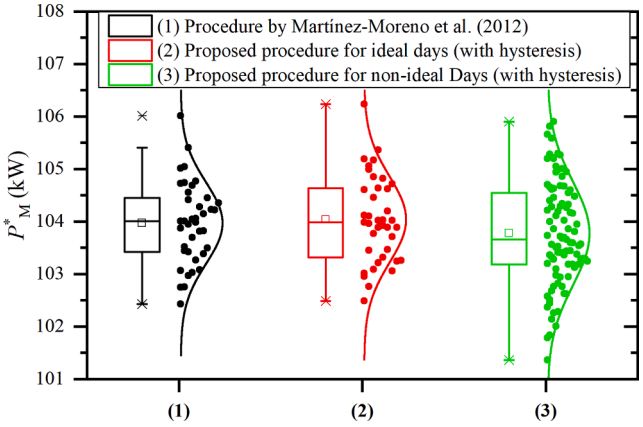

Fig. 10. Box plots of the nominal power values for every single day considering cases (1), (2), and (3) under analysis.

Table 2
Statistical analysis of the nominal power estimation procedures.

Case	Days	Median P^*_M (kW)	Mean P^*_M (kW)	Standard deviation (kW)	Q1 (kW)	Q3 (kW)	Q3-Q1 (kW)
Case (1): Martínez-Moreno et al. (2012); ideal conditions	39	104.00	103.97	0.77	103.42	104.45	1.03
Case (2): This work, ideal conditions with hysteresis data	39	103.98	104.04	0.82	103.32	104.64	1.32
Case (3): This work, non-ideal conditions	96	103.66	103.77	0.99	103.18	104.54	1.36

Gaussian or normal distribution, as also indicated by the very similar median and mean P^*_M values in Table 2. The latter indicates that for case (1), the mean of the P^*_M values is (103.97 ± 0.77) kW. The dispersion or uncertainty of the measurement is estimated by the interquartile range or IQR (Q3-Q1). This range represents the distribution of 50 % of the values. The respective IQR is 1.03 kW, indicating low uncertainty considering the installed power. Uncertainties between 2.5 % and 5 % have been reported in PV systems (Dirnberger et al., 2010:). In our case, the uncertainty presented in Table 2 does not exceed 0.5 %, even the standard deviation is 0.74 %. These low uncertainty values come mainly from uncertainty in the measurement of irradiance and temperature, which can be controlled only in laboratory conditions (Carullo et al., 2017).

For case (2) in Fig. 10, it can be seen that the daily P^*_M values are distributed in a similar range of values as in case (1). In Table 2, the mean P^*_M value of (104.04 ± 0.82) kW and IQR are both very similar to the values for case (1). These statistical metrics indicate that both procedures are statistically equivalent under these ideal conditions, thus validating the results of the non-parametric filter with the procedure used in (Martínez-Moreno et al., 2012).

Finally, for case (3) in Fig. 10, slightly higher dispersion of the daily P^*_M values are observed in comparison to the other two cases. In Table 2, this is observed in the slightly larger standard deviation and the IQR of 1.36 kW. This is expected due to some of the noise possibly affecting the mode, i.e., the most likely P^*_M value of the probability density function. Nevertheless, the mean P^*_M value of (103.77 ± 0.99) kW for case (3) is still within the ranges of the other two cases where one would be expecting to find the value of the nominal power of the PV plant (Ren et al., 2014).

Two aspects of the obtained results should be highlighted and summarized: On the one hand, both procedures find statistically indifferent mean values of nominal power value for clear sky days under ideal conditions. On the other hand, the non-parametric filter procedure estimates the effective nominal power without the need to eliminate non-linear data from the hysteresis effect.

7. Conclusions

This work proposes a new procedure to estimate the effective nominal power of a photovoltaic generator under outdoor conditions regardless of its size, resilient to particular monitoring challenges of large PV plants, and applicable even under non-ideal operational conditions. We validated the procedure by applying it to a PV plant of 109.40 kW nominal power under STC built and connected to the grid in 2008.

First, this PV plant presented a hysteresis effect due to the linear and non-linear behavior of the DC power data versus irradiance. The most likely causes of this effect were spatial inhomogeneities of module temperatures and the plane-of-array irradiance. The latter was due to inevitable string misalignments evidencing the challenges of monitoring large PV plants.

Second, non-ideal operating conditions on partially cloudy days caused noise in the DC power versus irradiance data, most likely due to partial shadowing in the PV generator. Standard characterization procedures for the PV nominal power are not applicable under such conditions. The new proposed procedure presents an advance in both regards, demonstrating robustness towards such monitoring challenges and non-ideal operating conditions.

The validation of the procedure was achieved through a continuous 135-day experimental campaign that applied high-precision instrumentation for monitoring. As a reference, the Martínez-Moreno et al. (Martínez-Moreno et al., 2012) procedure was applied to estimate the PV plant's nominal power, resulting in a mean daily nominal power of (103.97 ± 0.77) kW. It was applicable only in 29 % of the studied days, which offered ideal meteorological conditions (full clear sky). Furthermore, it required excluding non-linear data from the hysteresis effect.

The proposed procedure based on non-parametric statistics applied to these same days with ideal operating conditions resulted in a mean nominal power of (104.04 ± 0.82) kW, with no statistically significant difference to the reference. It is noteworthy that this new procedure did not require excluding non-linear data from the hysteresis effect.

Furthermore, applying the same non-parametric procedure to the remaining 71 % of monitoring days, which presented non-ideal conditions (partially cloudy sky), resulted in a mean nominal power of (103.77 ± 0.99) kW. This result is in good agreement with the previous results for ideal days. Therefore, the proposed non-parametric procedure is suitable for ideal and non-ideal operating conditions and can reliably estimate the effective nominal power for a single monitoring day.

Declaration of Competing Interest

The authors declare that they have no known competing financial interests or personal relationships that could have appeared to influence the work reported in this paper.

Acknowledgements

The authors thank Vlada Pleshcheva for her valuable comments on statistical analysis. This work received financial support by the Concytec – World Bank project "Mejoramiento y Ampliación de los Servicios del Sistema Nacional de Ciencia Tecnología e Innovación Tecnológica" 8682-PE, through its executing unit PROCIENCIA, contract N°045-2018-FONDECYT-BM-IADT-MU. José Angulo acknowledges the financial support given by Concytec under the Ph.D. scholarship program with contract N°236-2015-FONDECYT. The PUCP vicechancellorship for research also provided under the contract no. CAP-2021-A-0028/PI0737. Additionally, part of this work has been financed by the "Agencia Andaluza de Cooperación Internacional para el Desarrollo" of the Junta de Andalucía (Andalusian Autonomous Government), through the project "Emergiendo con el Sol" under expedient code 2012DEC026. Finally, the authors are grateful to the company GERION INGENIERIA for giving access to the facilities and permission for monitoring the PV plant.

References

Barykina, A., Hammer, A., 2017. Modeling of photovoltaic module temperature using Faiman model: Sensitivity analysis for different climates. Sol. Energy. 146, 401–416.
Carrillo, J.M., Martínez-Moreno, F., Lorenzo, C., Lorenzo, E., 2016. Uncertainties on the outdoor characterization of PV modules and the calibration of reference modules. Sol. Energy. 155, 880–892.
Carullo, A., Ferraris, F., Vallan, A., Spertino, F., Attivissimo, F., 2014. Uncertainty analysis of degradation parameters estimated in long-term monitoring of photovoltaic plants. Measurement 55, 641–649.
Carullo, A., Castellana, A., Vallan, A., Ciocia, A., Spertino, F., 2017. Uncertainty issues in the experimental assessment of degradation rate of power ratings in photovoltaic modules. Measurement 111, 432–440.

Chen, Y.C., 2017. A tutorial on kernel density estimation and recent advances. Biostat. Epidemiol. 1 (1), 161–187.
De la Parra, I., Muñoz, M., Lorenzo, E., García, M., Marcos, J., Martínez-Moreno, F., 2017. PV performance modelling: A review in the light of quality assurance for large PV plants. Renew. Sustain. Energy Rev. 2016 (78), 780–797.
Dirnberger, D., Bartke, J., Steinhüser, A., Kiefer, K., Neuberger, F., 2010. Uncertainty of field IV Curve measurements in Large Scale PV systems. 25th EU PVSEC. 6–10.
E2848 −13. Standard Test Method for Reporting Photovoltaic Non-Concentrator System. Reapproved 2018. 2013; 1–11.
Filik, U.B., Filik, T., Gerek, O.N., 2018. A hysteresis model for fixed and sun tracking solar PV power generation systems. Energies. 11 (3), 603.
Han, Q., Ma, S., Wang, T., Chu, F., 2019;115,:. Kernel density estimation model for wind speed probability distribution with applicability to wind energy assessment in China. Renew. Sustain. Energy Rev., 109387
Huang, B.J., Yang, P.E., Lin, Y.P., Lin, B.Y., Chen, H.J., Lai, R.C., et al., 2011. Solar cell junction temperature measurement of PV module. Sol. Energy. 85 (2), 388–392.
IEC 60904-3, 2008. Photovoltaic devices - Part 3: measurement principles for terrestrial photovoltaic (PV) solar devices with reference spectral irradiance data. Ed2.
IEC 61829, 2015. Photovoltaic (PV) array - On-site measurement of current-voltage characteristics. Ed2.
Irshad, J.Z.A., Haque, A., 2018. Temperature measurement of solar module in outdoor operating conditions using thermal imaging. Infrared Phys. Technol. 92, 34–138.
Jäger-waldau, A., 2021. Snapshot of Photovoltaics—March 2021. EPJ Photovoltaic. 12, 1–7.
Jäger-Waldau A. PV Status Report 2019. 2019, EUR 29938.
Jordan, D.C., Kurtz, S.R., 2013, 2013,. Photovoltaic degradation rates - An Analytical Review. Prog. Photovoltaics Res. Appl. 21 (1), 12–29.
Kelly, G., Spooner, T., Volberg, G., Ball, G., Bruckner, J., 2014. Ensuring the reliability of PV systems through the selection of international standards for the IECRE conformity assessment system. In: IEEE 40th Photovolt. Spec. Conf. PVSC 2014, pp. 914–918.
Kiefer, K., Reich, N.H., Dirnberger, D., Reise, C., 2011. Quality assurance of large scale PV power plants. In: Conf. Rec. IEEE Photovolt. Spec. Conf., pp. 001987–001992.
Kimber, A., Dierauf, T., Mitchell, L., Whitaker, C., Townsend, T., NewMiller, J., et al., 2009. Improved Test Method To Verify The Power Rating of a Photovoltaic (PV) Project. In: 2009 37th IEEE Photovoltaic Specialists Conference (PVSC), pp. 316–321.
Lomas, J.C., 2019. Propuesta de Una Nueva Metodologia de Analisis de Plantas FV Atendiendo a los Cambios Normativos Motivados por el RD 661/2007. Universidad de Jaen.
Lorente, D.G., Pedrazzi, S., Zini, G., Dalla Rosa, A., Tartarini, P., 2014. Mismatch losses in PV power plants. Sol. Energy. 100, 42–49.
Martínez-Moreno, F., Lorenzo, E., Muñoz, J., Moretón, R., 2012. On the testing of large PV arrays. Prog. Photovoltaics Res. Appl. 20 (1), 100–105.
Muñoz Escribano, M., Garcia Solano, M., De La Parra, L.I., Marcos Alvarez, J., Marroyo, L., Lorenzo, P.E., 2018. Module temperature dispersion within a large PV array: Observations at the amareleja PV plant. IEEE J. Photovoltaics. 8 (6), 1725–1731.
Muñoz, J.V., Nofuentes, G., Aguilera, J., Fuentes, M., Vidal, P.G., 2011. Procedure to carry out quality checks in photovoltaic grid-connected systems: Six cases of study. Appl. Energy. 88 (8), 2863–2870.
Muñoz, J.V., Nofuentes, G., Fuentes, M., de la Casa, J., Aguilera, J., 2016. DC energy yield prediction in large monocrystalline and polycrystalline PV plants: Time-domain integration of Osterwald's model. Energy. 114, 951–960.
Muñoz-Cerón, E., Lomas, J.C., Aguilera, J., de la Casa, J., 2018. Influence of Operation and Maintenance expenditures in the feasibility of photovoltaic projects: The case of a tracking pv plant in Spain. Energy Policy. 2017 (121), 506–518.
Navada, H.G., Singh, S.V., Shubhanga, K.N., 2017. Modelling of a Solar Photovoltaic Power Plant for Power System Studies. In: IEEE International Conference on Signal Processing, Informatics, Communication and Energy Systems (SPICES), pp. 1–6.
Nosratabadi, H., Mohammadi, M., Kargarian, A., 2019. Nonparametric Probabilistic Unbalanced Power Flow with Adaptive Kernel Density Estimator. IEEE Trans. Smart Grid. 10 (3), 3292–3300.
Polo, J., Fernandez-Neira, W.G., Alonso-García, M.C., 2017. On the use of reference modules as irradiance sensor for monitoring and modelling rooftop PV systems. Renew. Energy. 106, 186–191.
Quiroz, J.E., Stein, J.S., Carmignani, C.K., Gillispie, K., 2015. In-situ module-level I-V tracers for novel PV monitoring. IEEE 42nd Photovolt. Spec. Conf. PVSC 2015.
Rahman, M.M., Selvaraj, J., Rahim, N.A., Hasanuzzaman, M., 2018. Global modern monitoring systems for PV based power generation: A review. Renew. Sustain. Energy Rev. 82, 4142–4158.
Rawa, M.J.H., Thomas, D.W.P., Sumner, M., 2011. Simulation of non-linear loads for harmonic studies. Proceeding Int. Conf. Electr. Power Qual. Util. EPQU. 00037, 102–107.
Reich, N.H., Mueller, B., Armbruster, A., Van Sark, W.G.J.H.M., Kiefer, K., Reise, C., 2012. "Performance ratio revisited: is PR > 90 % realistic? Prog. Photovoltaics Res. Appl. 20 (6), 717–726.
Ren, Z., Yan, W., Zhao, X., Li, W., Yu, J., 2014. Chronological probability model of photovoltaic generation. IEEE Trans. Power Syst. 29 (3), 1077–1088.
Renewables 2021 Global Status Report. REN21. 2021.
Shiva Kumar, B., Sudhakar, K., 2015. Performance evaluation of 10 MW grid connected solar photovoltaic power plant in India. Energy Rep. 1, 184–192.
Tina, G.M., Ventura, C., Sera, D., Spataru, S., 2017. Comparative Assessment of PV Plant Performance Models Considering Climate Effects. Electr. Power Components Syst. 45 (13), 1381–1392.
Watts, J.L.R., Singh, R., Dross, F., 2017. Statistical analyses for capacity testing of photovoltaic systems. In: IEEE 44th Photovolt. Spec. Conf. PVSC 2017, pp. 1–5.
Whitfield, K., Osterwald, C.R., 2001. Procedure for determining the uncertainty of photovoltaic module outdoor electrical performance. Prog. Photovoltaics Res. Appl. 9 (2), 87–102.